A New Ground Fault Detection Method in Three-Wire Distribution Systems to Reduce Fire Hazards

Yanfeng Gong, Gandhali Prakash Juvekar, Normann Fischer, and Bill Glennon
Schweitzer Engineering Laboratories, Inc.

Jesse Rorabaugh, Juan Santillan, and Andrew Swisher
Southern California Edison

Presented at the
78th Annual Georgia Tech Protective Relaying Conference
Atlanta, Georgia
May 7–9, 2025

Previously presented at the
78th Annual Conference for Protective Relay Engineers at Texas A&M, March 2025

Originally presented at the
51st Annual Western Protective Relay Conference, October 2024

A New Ground Fault Detection Method in Three-Wire Distribution Systems to Reduce Fire Hazards

Yanfeng Gong, Gandhali Prakash Juvekar, Normann Fischer, and Bill Glennon,
Schweitzer Engineering Laboratories, Inc.
Jesse Rorabaugh, Juan Santillan, and Andrew Swisher,
Southern California Edison

Abstract—**A considerable number of three-wire ungrounded or resonant-grounded systems are in North America and a prevalence of even more are on other continents. On ungrounded or resonant-grounded systems, when a single-phase-to-ground fault occurs on a feeder, the fault current is significantly less compared to a multigrounded or solidly grounded feeder for the same fault and it cannot be reliably detected by conventional overcurrent protection. Utilities today face an urgency to employ rapid fault detection and isolation methods on such systems due to an increase in wildfire hazards. Faults generating even a few amperes can cause wildfires or severe public safety hazards if the faults are not isolated promptly. This challenge warrants a reliable solution for single-phase-to-ground fault detection in such systems. Existing fault detection methods, especially overcurrent-based methods, perform poorly because of the small fault current magnitude in the system.**

This paper presents a new single-phase-to-ground fault detection method that uses pure-fault current quantities, which eliminate the system load current effect. By using the identified unique relationship between pure-fault current characteristics of the faulted and unfaulted phases, the method detects single-phase-to-ground faults and reliably identifies the faulted feeder out of parallel feeders connected to the same bus. This method does not require any system parameters that are especially hard to obtain for distribution systems, allowing the method to be adapted to field reclosers. The associated number of settings used is minimal, and the values are easily obtained. This paper describes the method in detail and demonstrates its performance by using both actual fault events and staged system testing events.

I. Introduction

For power distribution, two types of systems are commonly used, namely three- or four-wire systems. When we refer to these systems as three- or four-wire systems, we are only counting the wires (conductors) that are designed to carry load current on the distribution system and we ignore the shield wire used to protect the distribution feeders from lightning. Three-wire power distribution systems are commonly used outside of North America to distribute electrical power to end users, but they also exist in the footprint of some utilities in North America. In these designs, the neutral is not brought outside the substation as a fourth wire and is either unigrounded via a neutral grounding resistor (NGR) or tunable reactor (Peterson coil) at the source substation or ungrounded. Unigrounded and ungrounded systems are even more popular than multigrounded systems in some parts of the world including most countries in Asia and Europe and in Australia.

For multigrounded and solidly unigrounded systems, ground fault current level is typically high and detectable by overcurrent protection unless the fault is a high-impedance fault. But for systems that are high-impedance unigrounded or ungrounded, the ground fault current may be undetectable by typical overcurrent protection as the return path for the ground current is via a high-impedance path. This low-magnitude fault current results in a very small change in the magnitude of the positive- and negative-sequence voltages, and therefore the phase-to-phase voltages are nearly unaffected. Because loads on these systems are connected phase-to-phase and a ground fault does not impact the phase-to-phase voltages on the system, loads are not impacted during a phase-to-ground fault on the system. Traditionally, such low fault currents during single-phase-to-ground faults were seen as an advantage of unigrounded and ungrounded systems, because there was no urgency to trip the line, and the systems continued to supply power without disrupting service to customers. But today, utilities face the challenge of detecting ground faults immediately even for such systems because a fault current of even a few amperes can ignite wildfires.

A ground fault on an ungrounded or unigrounded power system does increase the zero-sequence voltage magnitude of the power system. The increase in the zero-sequence voltage magnitude is inversely proportional to the magnitude of the fault resistance. The zero-sequence voltage magnitude on the power system is equal to the pre-fault phase-to-neutral voltage magnitude for a metallic fault, when the fault resistance is equal to zero. The increase in the zero-sequence voltage is in the opposite direction of the faulted phase pre-fault voltage. To detect the presence of a ground fault in an ungrounded or unigrounded system is not a challenge, this can be done by observing an increase in the magnitude of the zero-sequence voltage on the system. The challenge comes with detecting which feeder on the system is faulted and requires that the angle between the zero-sequence voltage and zero-sequence current be measured or calculated correctly [1].

For ungrounded systems, when a single-phase-to-ground fault occurs, the conductor touches the ground directly or indirectly and a very small amount of ground current flows. Fault current can only flow through the line-to-ground charging capacitance of the unfaulted phases and the other unfaulted lines connected to the same bus, which is still a high-impedance return path. The magnitude of the fault current is directly proportional to the sum of the charging capacitance of the unfaulted feeders operational on the power system. Ground fault detection methods such as zero-sequence voltage detection and sequence current relationship-based methods exist [2], but they are affected by factors like system standing unbalance and asymmetries that exist on the systems due to CTs and system configurations. Fault resistance from the conductor to ground also has a negative impact [1] [3]. As mentioned before, these methods lack inherent selectivity, and therefore they do not tell the user which feeder and phase have experienced the fault.

Compensated-grounded or resonant-grounded systems consist of an inductor (Peterson coil) connected to the neutral of the substation or source transformer. The typical goal of resonant-grounded systems is to compensate for the ground fault current flowing through the line-to-ground charging capacitances of the unfaulted phases to further reduce the fault current. To minimize the fault current, the inductor size is carefully selected to match the line-charging capacitance as closely as possible. However, connecting an inductor that fully compensates the line-to-ground charging capacitances of the unfaulted phases is impossible because of mismatches between the coil inductance and system shunt capacitance, shunt resistances which cannot be cancelled by the coil, coil resistances, system asymmetries, and availability. Resonant-grounded systems, therefore, tend to be over- or undercompensated, causing a small amount of fault current to flow. The fault current ranges from a few hundred milliamperes to a few amperes depending on the system configuration. Multiple methods exist in literature for detecting ground faults for compensated-grounded systems. The wattmetric method that uses the real component of the product of the zero-sequence voltage and current is commonly used for resonant-grounded systems but is also prone to misoperate because of the system standing unbalance, low zero-sequence current magnitude, and the requirement for supervision with zero-sequence voltage [4] [5].

Because resonant systems cannot completely compensate a system to reduce the fault current to near zero, utilities have adopted newer technologies for active compensation to fully eliminate ground fault current during single-phase-to-ground faults, especially for wildfire mitigation purposes. One of the well-known technologies is the Residual Current Compensator (RCC) that injects neutral current during faults so that the fault current, the majority of which is already compensated by the Peterson coil, is almost completely eliminated. When these methods detect the existence of faults, the utility may deploy mechanisms such as inserting a neutral earthing resistor to increase the ground fault currents for traditional protection methods to operate [3] [6]. This practice becomes undesirable under certain situations, such as a downed conductor, when trying to minimize the wildfire risks because large fault current will be introduced for the overcurrent protection. In such cases, a reliable ground fault method that does not cause hazardous situations, like the previously mentioned method does, is of utmost importance.

Additionally, employing compensation methods, such as the RCC that detects extremely high-impedance faults, requires reducing the level of background noise below a target level of sensitivity [6]. This noise can be a result of factors such as transformers connected from a phase to a multigrounded neutral, two-phase tap lines, asymmetrical phase construction, parallel transmission lines, and harmonics. Trying to minimize the impact of these factors through methods such as using capacitive balancing units can be a complicated and expensive task, with additional challenges to maintain a balanced distribution network over time. Despite the cost, time, and effort, the target fault detection sensitivity might not be achieved all the time because of these system imbalance effects. For such systems, a ground fault method that is unaffected by these factors can prove beneficial.

With this paper, we present a single-phase-to-ground fault detection solution that is suitable for ungrounded, resonant-grounded, and actively compensated-grounded systems. After studying a few commonly used methods, we determined that the solution needed to be agnostic of factors that affect other methods, such as system asymmetries, standing unbalance, and sensitivity. Using pure-fault quantities can help with these issues. Pure-fault quantities are quantities generated during a fault and are independent of the pre-fault system, i.e., existing load on the system does not impact these quantities. Active injection systems like the RCC normally take more than one cycle to evaluate and respond; pure-fault quantities are unaffected by these active compensation actions. The unique relationship between pure-fault quantities can help determine the existence of ground fault on resonant-grounded and ungrounded systems and provide high-speed fault detection in one power system cycle. The default settings suggested in this paper are applicable to most systems, significantly reducing the burden of fault studies usually required for other protection elements.

The rest of the paper is structured as follows. Section II describes the concept behind the method. Section III describes the implementation details for the method. In Section IV, we verify the proposed method through actual field data and discuss the results to demonstrate the effectiveness of this method.

II. Pure-Fault Quantities Relationship During a Single-Phase-to-Ground Fault

The proposed fault detection method uses a combination of pure-fault current components of the faulted feeder residual current and faulted-phase fault current to determine the specific feeder and phase involved in the ground fault. This ground fault detection can be qualified by zero-sequence voltage for security.

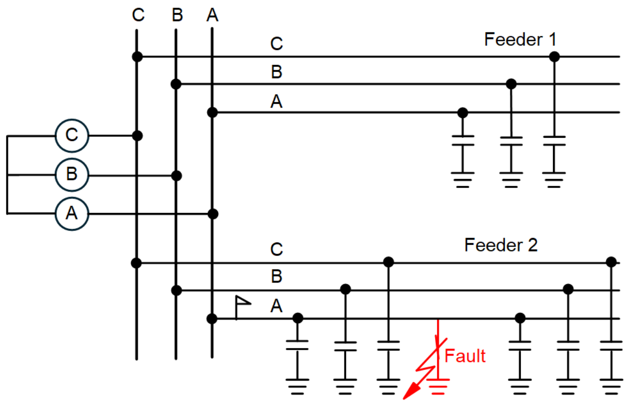

Fig. 1. Single-phase-to-ground fault on an ungrounded system.

Fig. 1 shows an ungrounded system with a fault on the A-phase of Feeder 2. The flag indicates the relay location. After a ground fault occurs on the system, as illustrated by Fig. 1, the fault network can be approximated by adding a reverse voltage source, V_f, at the fault point with fault resistance, as illustrated by Fig. 2, based on the superposition principle [7]. Fig. 2 shows the pure-fault circuit during a fault. This implies that the currents and voltages that the feeder relay measures during faults can be thought of as a summation of pre-fault and pure-fault quantities.

Using the above analysis:

Fault Network = Pre-Fault Network + Pure-Fault Network

Therefore:

Pure-Fault Network = (Fault Network) – (Pre-Fault Network)

The pure-fault network quantities, such as pure-fault currents, can be calculated by subtracting the pre-fault quantities, for example, one cycle before the fault, from the fault quantities that are measured by the relay at the present time.

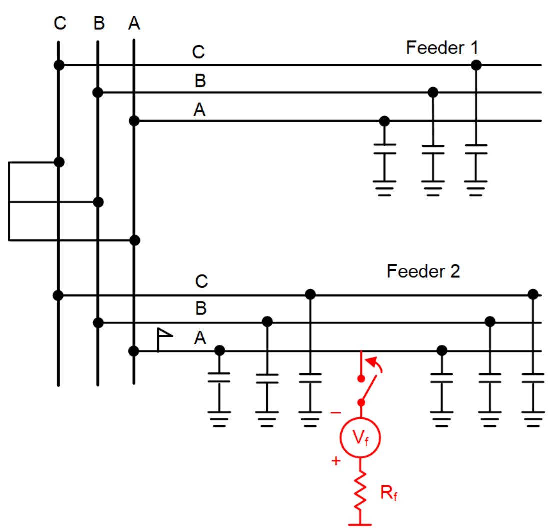

Fig. 2. Pure-fault circuit of a single-phase-to-ground fault on an ungrounded system.

Using the pure-fault network for single-phase-to-ground fault analysis of the system helps eliminate the effect of load current, standing unbalance, and other asymmetries in the system. The next two subsections detail the pure-fault system analysis for ungrounded and resonant-grounded systems.

A. *Ungrounded Systems*

When a ground fault occurs on an ungrounded system, as shown in Fig. 1, the steady ground fault current is very small because the fault current can only flow through the line-to-ground charging capacitances of the unfaulted phase. Due to existing ground current caused by system imbalance from factors mentioned earlier, detection and selection of the faulted feeder on which the single-phase-to-ground fault occurs is difficult. Immediately after the fault, transients may occur in the system because of the capacitive components (line-charging capacitances). Analyzing the pure-fault circuit helps identify unique relationships between pure-fault quantities during single-phase-to-ground faults.

Fig. 2 shows the pure-fault circuit of a two-feeder ungrounded system fed from a substation with a fault on the A-phase of Feeder 2. For the sake of analysis, this circuit can be simplified as shown in Fig. 3. If more than two feeders are connected to the same bus, the remaining unfaulted feeder can be lumped into the equivalent unfaulted feeders.

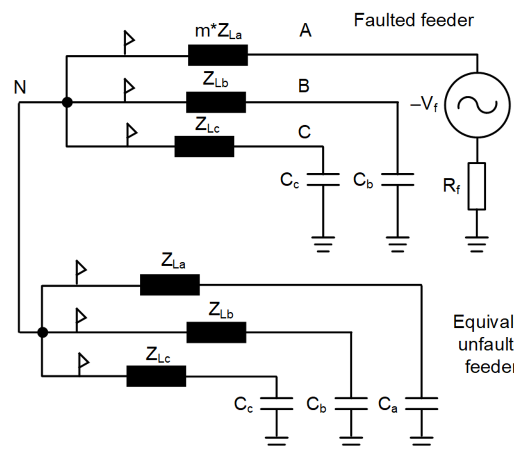

Fig. 3. Simplified pure-fault circuit of the feeder with a single-phase-to-ground fault on an ungrounded system.

V_F is the pre-fault voltage at the fault point right before the fault occurred, and R_F is the fault resistance. Let ΔI_A, ΔI_B, and ΔI_C be the pure-fault current measured by the relay on the A-phase, B-phase, and C-phase, respectively. Let I_F be the fault current flowing through R_F. The per-unit distance to the fault from the relay is m. For simplification, let ΔV_{BCap} and ΔV_{CCap} be the pure-fault voltage across the B- and C-phases line-to-ground charging capacitances. Then, apply Kirchoff's voltage law to Fig. 3 as follows:

$$-V_F + R_F \cdot I_F + \Delta I_A \cdot (m \cdot Z_{LA}) - \Delta I_B \cdot Z_{LB} = \Delta V_{BCap} \quad (1)$$

$$-V_F + R_F \cdot I_F + \Delta I_A \cdot (m * Z_{LA}) - \Delta I_C \cdot Z_{LC} = \Delta V_{CCap} \quad (2)$$

Simplifying (1) and (2):

$$-V_F + V_{drop-others} = \Delta V_{BCap} \quad (3a)$$

$$-V_F + V_{drop-others} = \Delta V_{CCap} \quad (3b)$$

where:

$$V_{drop-others} = R_F \cdot I_F + V_{line-drop} \quad (4)$$

Except for the $V_{drop-others}$ in (4), most of the inverted fault voltage appears across the B- and C-phases line-to-ground charging capacitances. For a typical distribution feeder that has aluminum conductors, the impedance for a 10-mile line could range between 2.5 ohms and 10 ohms. The pure-fault current quantities are small, depending on the length of the feeder and feeder type. As a result, when compared to V_F (7.2 kV for a 12.47 kV system), the line-drop voltage ($V_{line-drop}$) is small. Therefore, $V_{drop-others}$ is small when R_F is small.

For the unfaulted phases, assuming $C_b = C_c = C$:

$$\Delta I_B = \Delta I_C = C\frac{d(-V_F + V_{drop-others})}{dt} \quad (5)$$

Equation (5) is applicable to all the unfaulted phases of the faulted feeder as well as all phases of all nonfaulted feeders connected to the same bus.

By using the analysis of Fig. 3, we can determine the direction of pure-fault current, as shown in Fig. 4. The magnitude of pure-fault current flowing through the faulted phase conductor is the highest because it is the result of the cumulative pure-fault current of the nonfaulted phases of the faulted feeder and pure-fault current of all the phases of the unfaulted feeders connected to the same bus, as described by (6):

$$\Delta I_A = -\left(\Delta I_B + \Delta I_C + \sum_{n=1}^{f} \Delta I_{ph,n}\right) \quad (6)$$

where:

f is the number of feeders

ph = A, B, or C

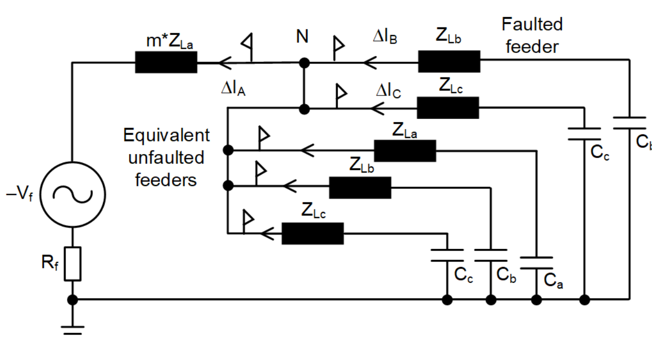

Fig. 4. Direction of current using analysis of Fig. 3.

The zero-sequence pure-fault current of the faulted feeder is the highest, being the superposition of the zero-sequence fault current of other unfaulted feeders (7):

$$\Delta 3I_0 = \Delta I_A + \Delta I_B + \Delta I_C$$
$$\Delta 3I_{0-faulted} = -\left(\sum_{n=1}^{f} \sum_{unfaulted,ph} \Delta I_{ph,n}\right) \quad (7)$$

For the unfaulted feeders, the zero-sequence pure-fault current is smaller compared to the faulted feeder, as described by (8):

$$\Delta 3I_{0-unfaulted} = 3C\frac{d(-V_F + V_{drop-others})}{dt} \quad (8)$$

It should be noted from (4) and (5) that noticeable pure-fault currents circulate in the system post fault when the $V_{drop-others}$ is at a minimum. If the fault resistance, R_F, is too high (in the order of thousands of ohms), the pure-fault currents may become indetectable. Equations (4) and (5) show that the magnitude of the pure-fault phase currents, ΔI_B and ΔI_C, depends on the voltage change across the line-ground charging capacitance. These equations influence $V_{line-drop}$, which is a few hundred volts and is a relatively small portion of $V_{drop-others}$. Therefore, if the fault resistance, R_F, is high, the $V_{drop-others}$ term is high and the change in voltage across these capacitors ($= -V_F + V_{drop-others}$) immediately after the fault is small, causing negligible ΔI_B and ΔI_C.

B. Resonant-Grounded Systems

When a ground fault occurs on a resonant-grounded system, as illustrated in Fig. 5, the steady ground fault current may be very small, depending on how much the system is compensated. Immediately after the fault, transients may occur in the system because of the inductive (Peterson coil) and capacitive components (line-charging capacitors). As mentioned earlier, analyzing the pure-fault circuit helps identify unique relationships between pure-fault quantities during single-phase-to-ground faults. Certain installations of resonant-grounded circuits may employ Rapid Earth Fault Current Limiter (REFCL) technologies like the RCC (as shown in Fig. 5) in conjunction with the traditional Peterson coil (or arc suppression coil) to compensate the system fully during a single-phase-to-ground fault. This method allows driving the fault current to zero to reduce wildfire hazards [8] or leaving loads online for extended times with a fault on the system [9]. These systems have fast response times but still require at least one power cycle for the system to detect and start compensating. The proposed pure-fault quantities-based algorithm is designed to operate within a cycle. Hence, equipment injecting currents by using inverters or compensating residual current by other means does not have an impact on the working of these methods, as depicted in Fig. 5. The active compensation component can be thought of as equivalent to closing a grounding switch on the faulted phase at the point of the fault a few cycles after the fault occurs. Therefore, the performance of the proposed fault detection method is not affected by the existence of an RCC.

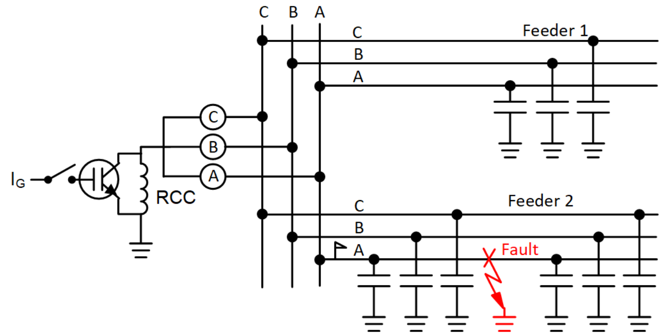

Fig. 5. Single-phase-to-ground fault on a resonant-grounded system.

Fig. 5 shows the pure-fault circuit of a two-feeder resonant-grounded system fed from a substation with a fault on the A-phase of Feeder 2. For the sake of analysis, this circuit can be simplified to the one shown in Fig. 6.

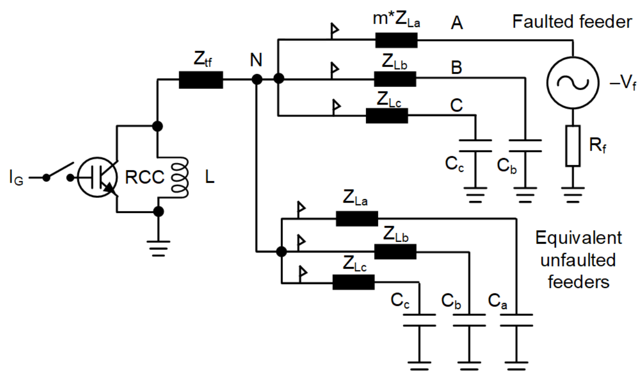

Fig. 6. Simplified pure-fault circuit of the feeder with a single-phase-to-ground fault on a resonant-grounded system.

Using the same notations as the ungrounded system, we made the following analysis:

$$-V_F + R_F \cdot I_F + \Delta I_A \cdot (m \cdot Z_{LA}) - \Delta I_B \cdot Z_{LB} = \Delta V_{BCap} \quad \text{same as (1)}$$

$$-V_F + R_F \cdot I_F + \Delta I_A \cdot (m \cdot Z_{LA}) - \Delta I_C \cdot Z_{LC} = \Delta V_{CCap} \quad \text{same as (2)}$$

$$-V_F + V_{drop-others} = \Delta V_{BCap} \quad \text{same as (3a)}$$

$$-V_F + V_{drop-others} = \Delta V_{CCap} \quad \text{same as (3b)}$$

where:

$$V_{drop-others} = R_F \cdot I_F + V_{line-drop} \quad \text{same as (4)}$$

As analyzed in ungrounded systems, most of the inverted fault voltage appears across the unfaulted B- and C-phases line-to-ground charging capacitances. Assuming $C_b = C_c = C$:

$$\Delta I_B = \Delta I_C = C \frac{d(-V_F + V_{drop-others})}{dt} \quad \text{same as (5)}$$

Equation (5) is applicable to all the unfaulted phases of all feeders connected to the same bus.

Let ΔV_{NG} be the pure-fault voltage across the arc suppression coil, Z_{tf} be the transformer impedance, and ΔI_{NG} be the pure-fault current flowing through it:

$$\Delta V_{NG} - \Delta I_{NG} \cdot Z_{tf} = \Delta I_A \cdot (m \cdot Z_{LA}) - V_F + R_F \cdot I_F$$

Therefore:

$$-V_F + V_{drop-others} = \Delta V_{NG}$$

The $\Delta I_{NG} \cdot Z_{tf}$ term is negligible and can be ignored. Similar to the analysis for ungrounded systems, without the voltage drop, most of the inverted fault voltage appears across neutral-to-ground-connected Peterson coil. Use (9) to obtain the pure-fault inductor current:

$$\int \left(\frac{\Delta V_{NG}}{L}\right) dt = \Delta I_{NG}$$
$$\int \left(-V_F + \frac{V_{drop-others}}{L}\right) dt = \Delta I_{NG} \quad (9)$$

By using the analysis for Fig. 6, we can determine the direction of pure-fault current, as shown in Fig. 7. The magnitude of the pure-fault current flowing through the faulted phase conductor is the highest because it is the cumulative result of the following:

- The pure-fault current of the nonfaulted phases of the faulted feeder
- The pure-fault current of all the phases of the unfaulted feeders connected to the same bus
- The pure-fault current flowing through the inductor (from (9))

$$\Delta I_A = -\left(\Delta I_B + \Delta I_C + \sum_{n=1}^{f} \Delta I_{ph,n} + \Delta I_{NG}\right) \quad (10)$$

where:

f is the number of feeders

ph = A, B, or C

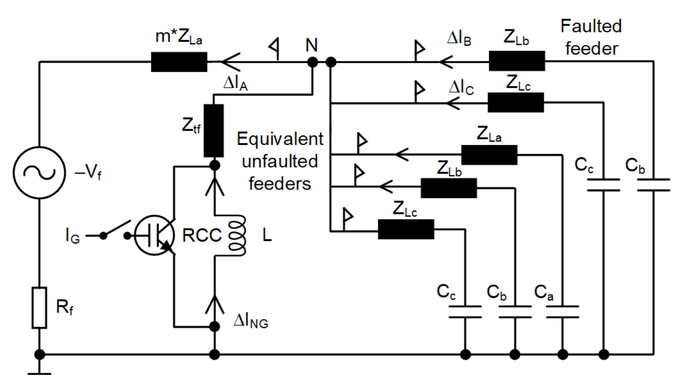

Fig. 7. Direction of current using analysis of Fig. 6.

Like ungrounded systems, the zero-sequence pure-fault current of the faulted feeder is the highest because it is a superposition of the zero-sequence pure-fault currents of other unfaulted feeders, as described in (7). Similarly, the zero-sequence pure-fault currents of unfaulted feeders are much smaller than the zero-sequence current of the faulted feeder, as described in (8).

Similar to the analysis of the ungrounded systems, the assumptions made in the analysis are valid when the

$V_{drop-others}$ is minimal. Extremely high fault resistance R_F has an impact on the pure-fault current magnitude and the performance of this algorithm.

Lastly, for both resonant-grounded and ungrounded systems, zero-sequence voltage, $3V_0$, is a reliable indicator of the existence of a single-phase-to-ground fault on the system, except for very high fault impedance that causes only a small change in the faulted phase voltage. Using 20 percent of the system nominal voltage as the $3V_0$ pickup threshold provides good fault resistance coverage for a single-phase-to-ground fault.

$$3V_0 = V_{AG} + V_{BG} + V_{CG} \quad (11)$$

III. Detection Algorithm

This section describes the fault detection process and outlines the thresholds used in the algorithm. Fig. 8 shows the logic diagram of the proposed single-phase-to-ground fault detection method. The pure-fault quantities are computed by using one-cycle-old quantities, i.e.:

$$\Delta\text{quantity} = \text{quantity}_t - \text{quantity}_{t-1} \quad (12)$$

The currents and voltages are filtered to extract the fundamental frequency quantities. Because of the filtering effect, the pure-fault quantities often exist for slightly longer than one cycle.

A. Pure-Fault Residual Current Check

The logic checks the pure-fault residual current ($\Delta 3I_0$) to identify whether a fault may be on the feeder. As described in Section II, pure-fault residual current magnitude increases immediately at the fault point after the fault occurs on the feeder. If the rise is higher than the current detection threshold for the monitored feeder, the check criterion passes, as seen in Fig. 8. The setting for this check can be made based on distribution voltage level, length of the feeders, number of feeders, and the type of grounding configuration: resonant-grounded or ungrounded. Ungrounded systems require lower setting values compared to resonant-grounded systems with similar system parameters. Lower feeder lengths and lower system voltage mean lower pure-fault residual current after a fault, and the setting should be lowered accordingly. Obtain the minimum threshold by examining the salient noise and setting the threshold higher than the noise level plus some margin. If highly sensitive neutral current inputs are available in relays, they should be used. To confirm that the method is not picking up noise, set a pickup duration of 0.5 cycles for the criterion to pass. For the next check to pick up correctly before the pure-fault residual current quantity disappears, a timer dropout of 0.5 cycles is set.

B. Phase Pure-Fault Current Check

After the pure-fault residual current check is satisfied, the logic checks the phase pure-fault currents (ΔI_A, ΔI_B, and ΔI_C) to confirm the fault. As detailed in Section II, the faulted phase pure-fault current magnitude is the highest compared to the unfaulted phases. In theory, the pure-fault current of the faulted phase is in the opposite direction of the pure-fault current of the two unfaulted phases. The pure-fault current phase angle information of each phase can be used for the decision to improve security. However, in practicality, the pure-fault current of the two unfaulted phases are in the range of amperes or subamperes in primary. Considering the current transformer (CT) ratio and device measurement accuracy, the phase angle information of the two unfaulted phases is not necessarily stable, and therefore the phase angle information is not reliable all the time. We propose a new pure-fault current comparison logic. We obtain the maximum and the median magnitude values of three-phase pure-fault currents. The logic determines if the maximum value is greater than three times the median value to filter out a line-switching disturbance, and the logic only picks up on a single-phase-to-ground fault. The logic also determines if the magnitude of the maximum phase pure-fault current is greater than the current detection threshold. To ensure that the method is not picking up on noise, a pickup duration of 0.5 cycles is set for the criterion to pass. When this check passes, a single-phase-to-ground fault alarm asserts.

It may take the zero-sequence voltage a few cycles to reach the pickup threshold if the fault starts with a very high fault resistance value. Therefore, we want to latch the phase pure-fault current check result for a bit longer to give enough time for $3V_0$ to pick up. A recommended default dropout time delay is 5 cycles.

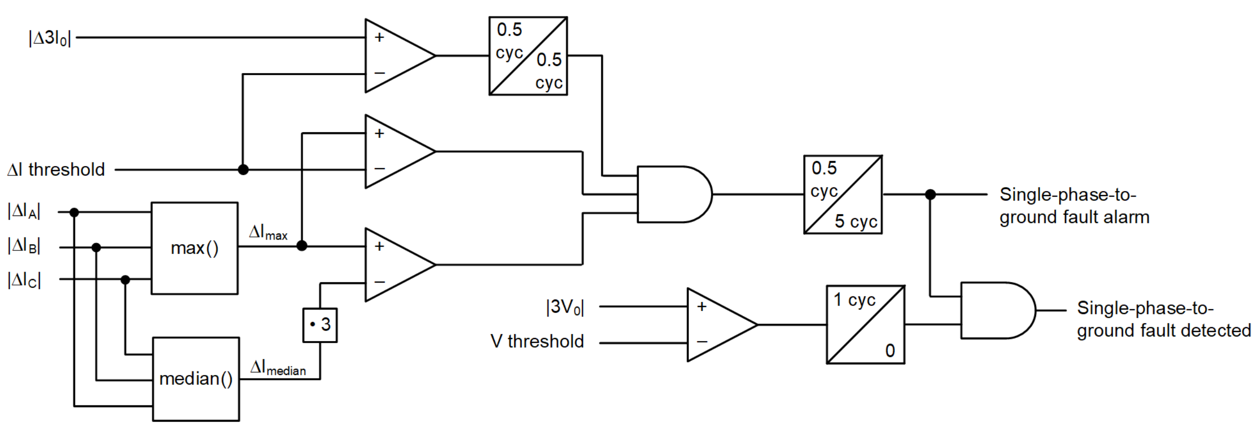

Fig. 8. Logic flowchart of the proposed single-phase-to-ground fault detection method.

C. *Zero-Sequence Voltage Detection*

As mentioned in Section II, the zero-sequence voltage at the bus is elevated during a single-phase-to-ground fault in both resonant-grounded and ungrounded systems.

As the faulted phase touches a ground through a fault resistance, the voltage of the faulted phase decreases. This decrease is dependent on the fault resistance and results in increasing the zero-sequence voltage, as seen in (11). If this zero-sequence voltage increases beyond the voltage detection threshold, the check passes as described in Fig. 8. A typical setting of 20 percent of the system nominal voltage works for most cases. A lower setting can be used for increased sensitivity, although sensitivity is also dependent on the network system capacitance.

When all three criteria pass, a single-phase-to-ground fault is detected. The faulted phase is the one that has the maximum pure-fault current. The residual fault current may increase for a parallel unfaulted feeder, but the pure-fault current check logic should block the unfaulted feeder from declaring a single-phase-to-ground fault.

IV. Results

This section shows three field events from ungrounded and resonant-grounded systems that test the validity of the proposed single-phase-to-ground fault detection method. One event report is for an ungrounded system with an unknown fault resistance. Two staged events are for resonant-grounded systems with 225 ohms fault resistance for an overhead line fault and an underground cable fault.

A. *B-Phase-to-Ground Fault on an Overhead Feeder in an Ungrounded System*

This is an actual event that occurred on an ungrounded, 4.8 kV system at a U.S. utility. Fig. 9 shows the raw voltage (a), raw current (including load current) (b), and filtered pure-fault current (< 5A) (c) waveforms during the fault. The phase currents do not strongly indicate a fault on the circuit or even a faulted phase. The fundamental pure-fault current waveform shows a jump in the faulted phase.

We implemented the method detailed in Fig. 8 to validate our analysis. The zero-sequence voltage detection threshold of 20 percent of nominal line-to-line voltage is used, but a much more sensitive current threshold of 1.5 A is used because the length of the feeders is short, and therefore the summation result of the charging current is small, requiring a lower current threshold. Analyzing Fig. 10 for this fault, we observe in Fig. 10(a) that the feeder pure-fault residual current magnitude is higher than the detection threshold, indicating that a fault may be on the feeder.

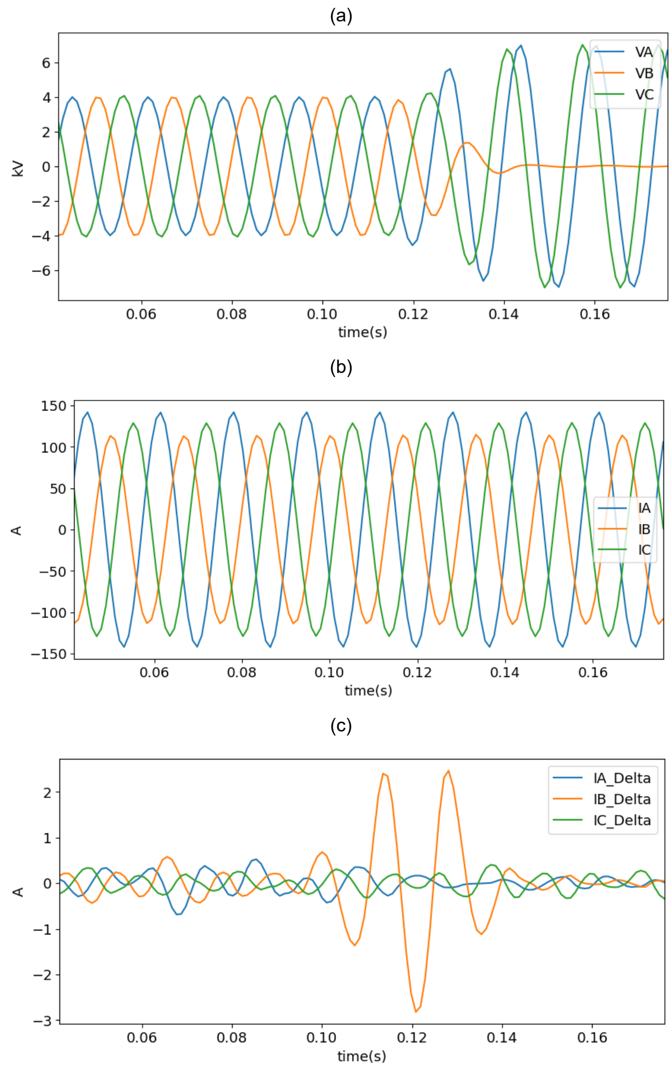

Fig. 9. Voltage (a), current (b), and pure-fault current (c) waveforms for the fault.

Next, we see in Fig. 10(b) that the pure-fault phase current magnitude is the highest for the B-phase and is greater than three times the median pure-fault phase current quantity on that feeder, which clearly indicates the ground fault is on this feeder and on the B-phase. The zero-sequence voltage magnitude crosses the detection threshold within a couple of cycles after the fault, as seen in Fig. 10(c). After picking up for 1 cycle, the logic confirms the single-phase-to-ground fault on the B-phase of the feeder.

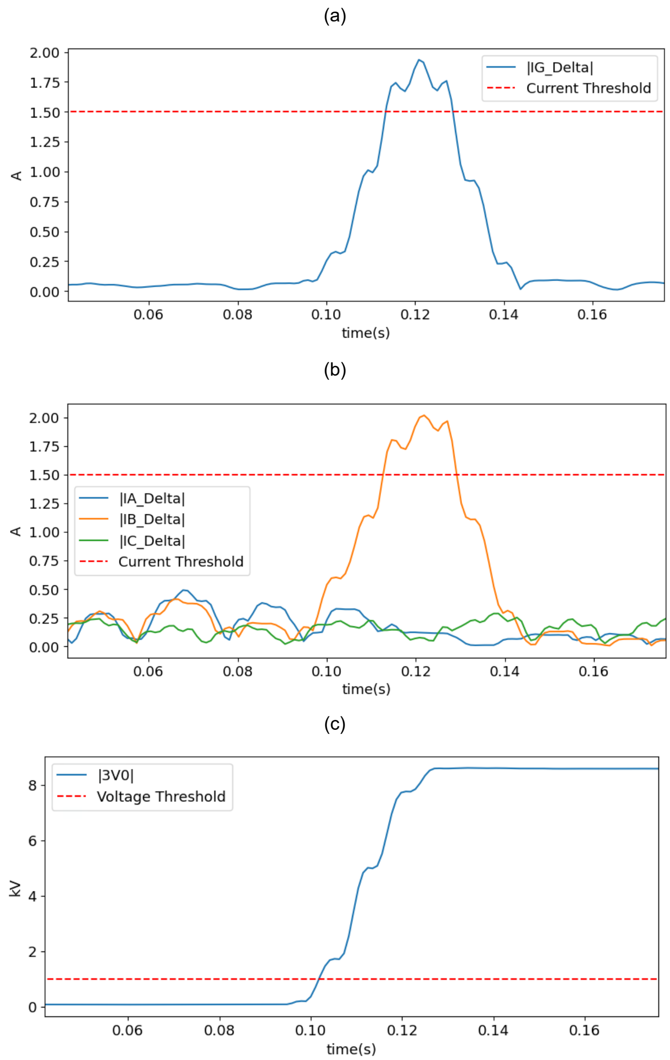

Fig. 10. Pure-fault residual currents of all feeders (a), pure-fault phase currents of the faulted feeder (b), and zero-sequence voltage at the bus (c).

B. B-Phase-to-Ground Fault on an Overhead Feeder in a Resonant-Grounded System

This event occurred on the end of the line on Feeder 2 in a resonant-grounded system with REFCL technology adopted through an RCC system. All three feeders connected to the bus, Feeder 1, Feeder 2, and Feeder 3, have similar lengths. Feeder 3 is an underground cable and naturally has higher line-to-ground charging capacitance. A 225-ohm fault was induced on the B-phase of Feeder 2 during a staged test.

Fig. 11 shows the voltage, current, and pure-fault current waveforms during the fault. The faulted B-phase experiences a slight increase in phase current for about two cycles, but not enough for any overcurrent protection to operate. The pure-fault current waveform shows a jump in faulted phase pure-fault current for a cycle with a distinct or sharp change in the following cycle, likely because of the RCC technology operating after a delay.

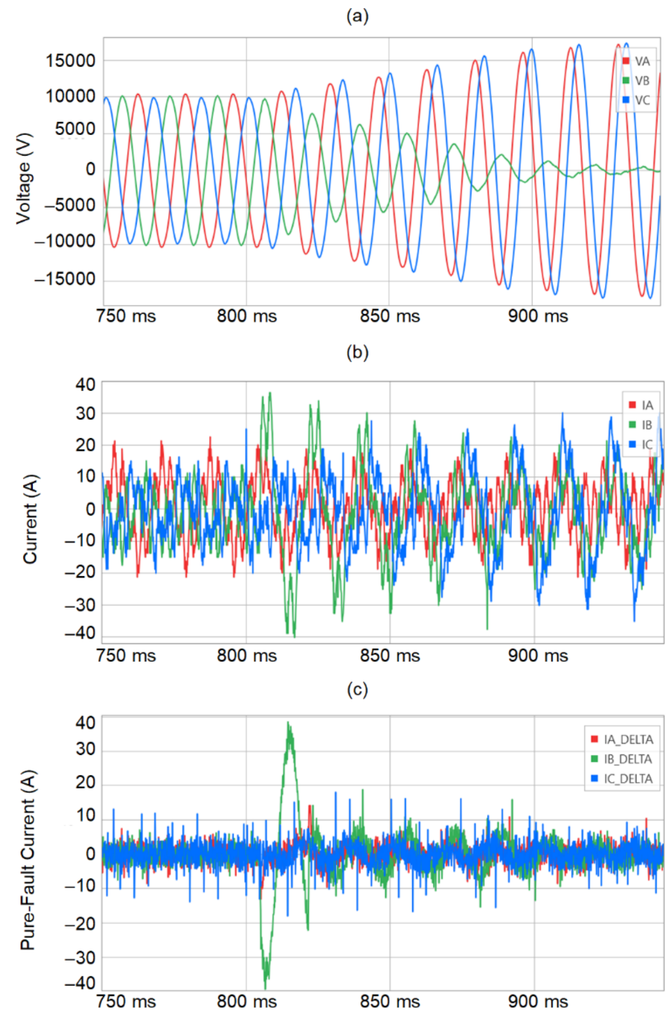

Fig. 11. Voltage (a), current (b), and pure-fault current (c) waveforms for the fault.

Similar to the previous event, we used the logic in Fig. 8 to analyze this event. The zero-sequence voltage detection threshold was set at 20 percent of nominal line-to-line voltage, and the current detection threshold was set at 5 A primary. The pickups and dropouts mentioned in Section III were used.

Analyzing Fig. 12 for this fault, we observe in Fig. 12(a) that the Feeder 2 pure-fault residual current magnitude is higher than the detection threshold, indicating that the fault may be on Feeder 2. Because, Feeder 3 is an underground cable of comparable length to Feeder 2, the fault residual current magnitude may be higher for Feeder 3, but the pure-fault residual current magnitude is highest for the faulted feeder. This illustrates the benefit of using the pure-fault current.

Next, we see in Fig. 12(b) that the pure-fault phase current magnitude is highest for the B-phase and is greater than three times the median pure-fault phase current quantity on that feeder, which clearly indicates the ground fault is on Feeder 2. For comparison, the pure-phase currents for unfaulted Feeder 1 are all lower than the detection threshold, as seen in Fig. 12(c).

The zero-sequence voltage magnitude crosses the detection threshold within a couple of cycles after the fault, as seen in Fig. 12(d). After picking up for 1 cycle, the logic confirms the single-phase-to-ground fault on the A-phase of Feeder 2.

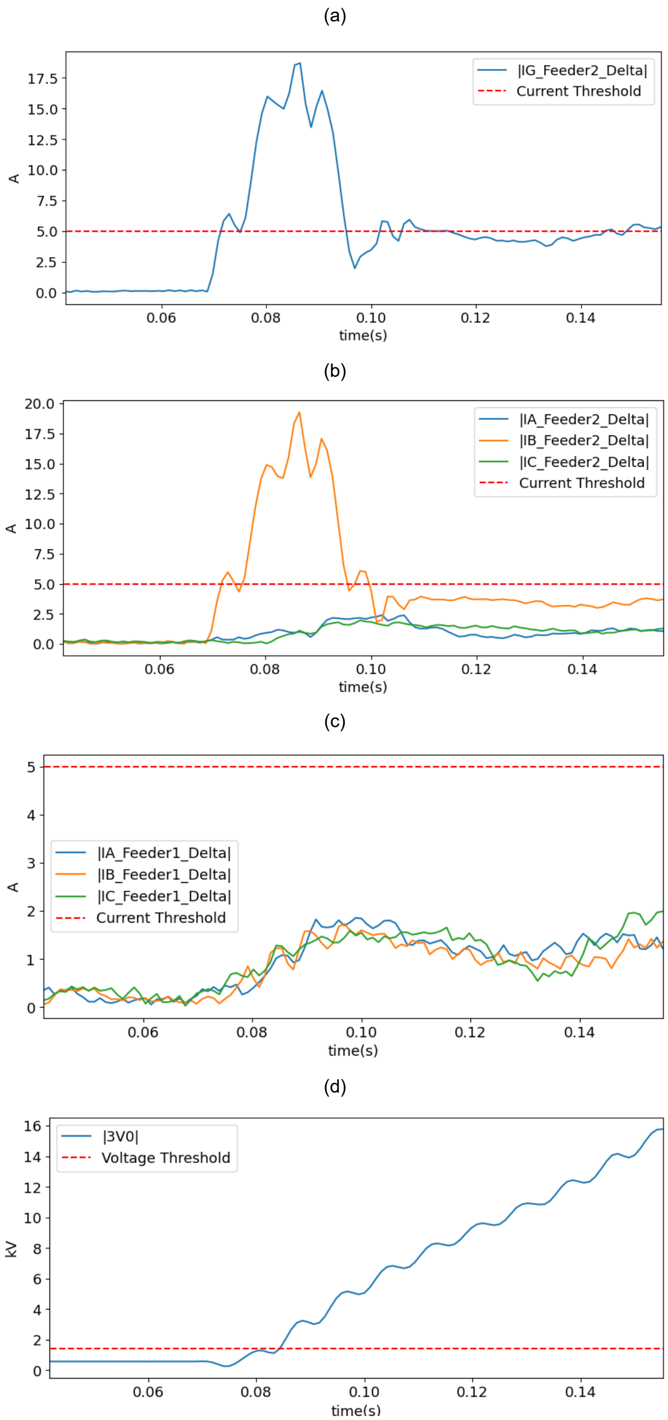

Fig. 12. Pure-fault residual currents of all feeders (a), pure-fault phase currents of the faulted feeder (b), pure-fault phase currents of an unfaulted feeder (c), and zero-sequence voltage at the bus (d).

C. C-Phase-to-Ground Fault on an Underground Cable Feeder in a Resonant-Grounded System

The staged event occurred on Feeder 3 in the same circuit as the fault in Subsection IV.B. This fault was a close-in, 225-ohm fault on the C-phase of Feeder 3. Note that although the fault was on the C-phase, which can be seen from the C-phase voltage drop, currents for all three phases vary with similar magnitude, demonstrating again that checking only the fault currents may not help with fault detection.

Fig. 13 shows the voltage (a), current (b), and pure-fault current (c) waveforms during the fault. The faulted C-phase experiences a slight increase in phase current, but so does the A-phase, making it hard to be selective by using just normal phase currents. In contrast, the pure-fault current waveform shows a jump in the faulted phase pure-fault current for a cycle with a distinct or sharp change in the following cycle, likely because of the RCC technology operating after a delay.

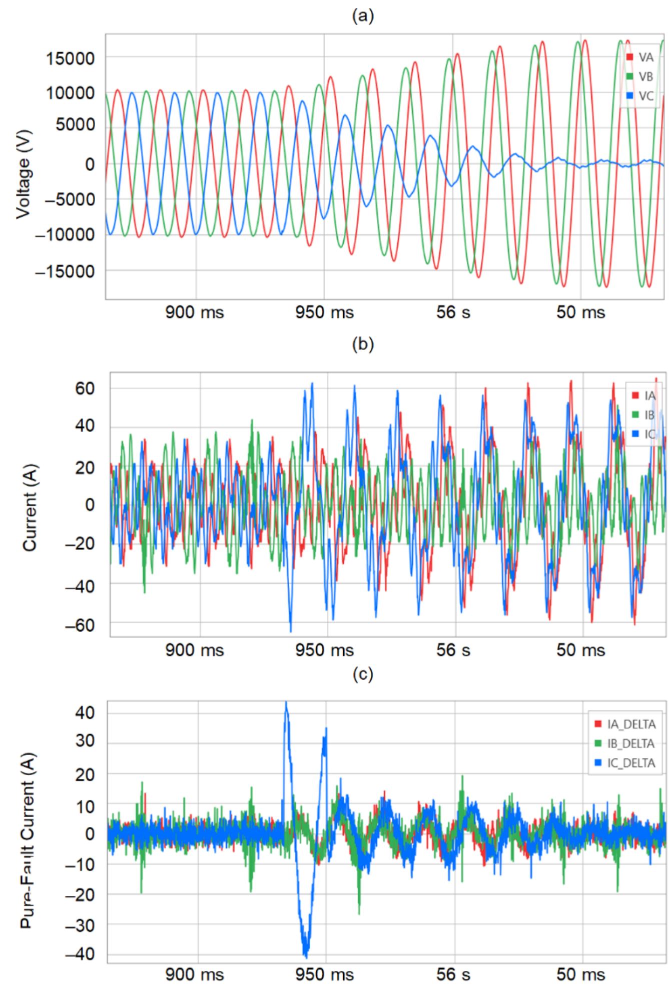

Fig. 13. Voltage (a), current (b), and pure-fault current (c) waveforms for the fault.

Similar to the previous event, we used the logic in Fig. 8 to analyze this event. The same settings as the last event were used. Analyzing Fig. 14 for this fault, we observe in Fig. 14(a) that the Feeder 3 pure-fault residual current magnitude is higher than the detection threshold, indicating that there may be a single-phase-to-ground fault on Feeder 3.

Next, we see in Fig. 14(b) that the pure-fault phase current magnitude is highest for the C-phase and is greater than three times the median pure-fault phase current quantity on that feeder. For comparison, the pure-phase current magnitudes for unfaulted Feeder 2 are all lower than the detection threshold, as seen in Fig. 14(c).

The zero-sequence voltage magnitude crosses the detection threshold within a couple of cycles after the fault, as seen in Fig. 14(d). After picking up for 1 cycle, the logic confirms the single-phase-to-ground fault on the A-phase of Feeder 3.

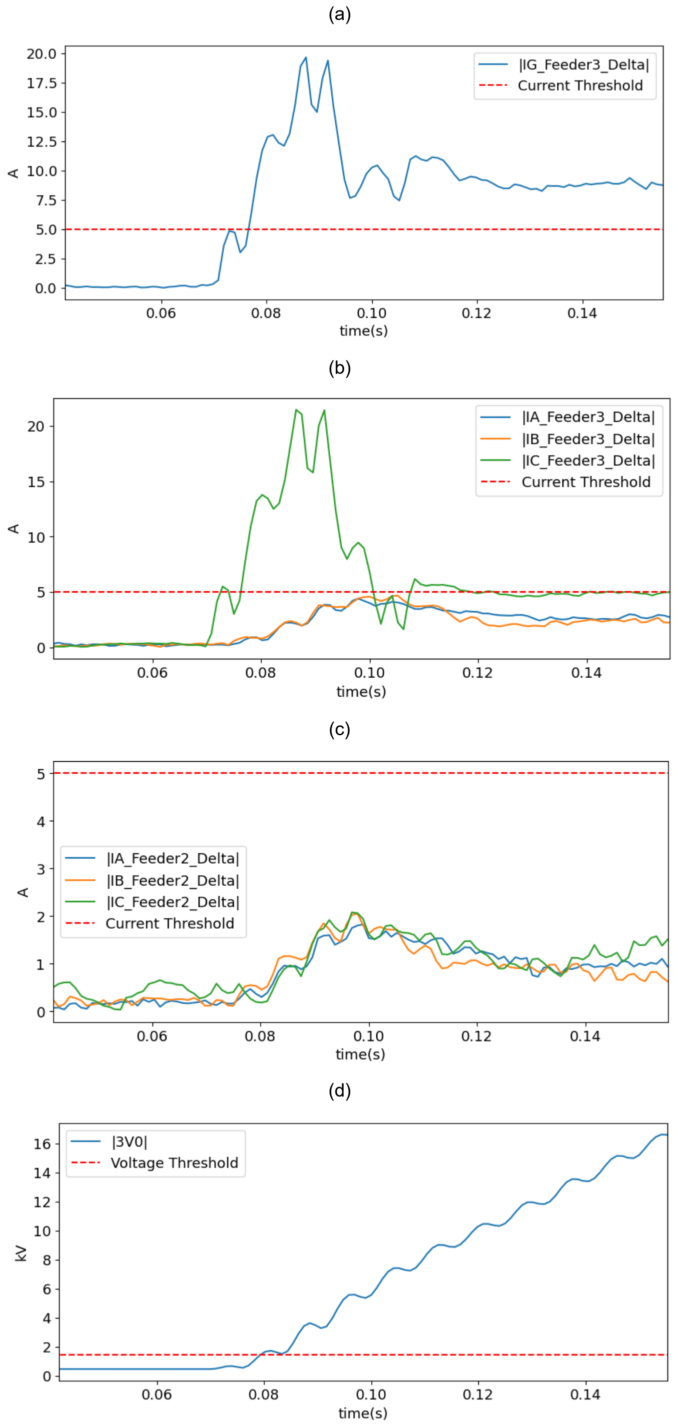

Fig. 14. Pure-fault residual currents of all feeders (a), pure-fault phase currents of the faulted feeder (b), pure-fault phase currents of an unfaulted feeder (c), and zero-sequence voltage at the bus (d).

V. Conclusion

Detecting single-phase-to-ground faults in power distribution systems with ungrounded or compensated grounding schemes has often been overlooked in the past because these system faults result in low fault currents. However, in today's environment, especially in regions where wildfire is a high risk, even the small fault currents resulting from these three-wire, unigrounded, and ungrounded systems are potent enough to start a fire if the fault is not cleared promptly. In general, leaving a single-phase-to-ground fault uncleared can be a public safety hazard, and maximizing the reliable fault detection sensitivity can minimize these hazards.

This paper presents an innovative and effective method to reliably detect single-phase-to-ground faults in ungrounded, resonant-grounded, or actively compensated grounded distribution systems. This method has the following characteristics, making it suitable for implementation in distribution feeder relays and line recloser controls:

- It relies only on the local measurement to determine whether the single-phase-to-ground fault is in front of the relay or not.
- It is unaffected by the existing load unbalance or CT measurement asymmetries because it uses delta or pure-fault quantities.
- Its default settings for 3V0 pickup and delta current pickup make it suitable for most applications and an almost settingless protection element.

As the industry deploys various technologies, including changing the distribution feeder grounding schemes to mitigate fire risks caused by power lines, the authors contribute this new proposed method to reduce fire risks, enhance public safety, and improve electricity service reliability.

VI. References

[1] D. Hou and N. Fischer, "Deterministic High-Impedance Fault Detection and Phase Selection on Ungrounded Distribution Systems," 2006 Power Systems Conference: Advanced Metering, Protection, Control, Communication, and Distributed Resources, Clemson, SC, USA, 2006, pp. 112–122.

[2] J. Roberts, H. J. Altuve, and D. Hou, "Review of Ground Fault Protection Methods for Grounded, Ungrounded, and Compensated Distribution Systems," proceedings of the 28th Annual Western Protective Relay Conference, Spokane, WA, October 2001, pp. 1–40.

[3] D. Hou, "Comparing Fault Resistance Coverage of Different Distribution System Grounding Methods," proceedings of the 37th Annual Western Protective Relay Conference, Spokane, WA, October 2010.

[4] AIEE Committee Report, "Sensitive Ground Protection," AIEE Transactions, Vol. 69, 1950, pp. 473476.

[5] E. T. B. Gross, "Sensitive Fault Protection for Transmission Lines and Distribution Feeders," AIEE Transactions, Vol. 60, Nov. 1941, pp. 968972.

[6] J. Rorabaugh, N. Rexwinkel, and A. W. Fresquez, "Rapid Earth Fault Current Limiter (REFCL) Projects at Southern California Edison." Available: sce.com.

[7] G. Benmouyal and J. Roberts, "Superimposed Quantities: Their True Nature and Application in Relays." proceedings of the 26th Annual Western Protective Relay Conference, Spokane, WA, October 1999.

[8] "REFCL Functional Performance Review." Available: energysafe.vic.gov.au.

[9] K. M. Winter, "The RCC Ground Fault Neutralizer—A Novel Scheme for Fast Earth-Fault Protection," CIRED 2005—18th International Conference and Exhibition on Electricity Distribution, Turin, Italy, 2005.

VII. Biographies

Yanfeng Gong earned his BS in Electrical Engineering with a focus on power systems from Wuhan University, China, in 1998. He then went on to obtain his MSEE from Michigan Technological University in 2002 and his PhD from Mississippi State University in 2005, continuing his specialization in power systems. Yanfeng worked as a research engineer at Schweitzer Engineering Laboratories, Inc. (SEL) from 2005 to 2013. He served as a principal engineer and supervisor at American Electric Power (AEP) in the Advanced Transmission Studies & Technologies (ATST) department from 2013 to 2019. In 2019, he returned to SEL, assuming the role of principal engineer. In addition to his professional endeavors, Yanfeng has played an active role in industry committees. He served as the past chair of the IEEE Transient Analysis and Simulation Subcommittee (TASS) and is currently the vice chair of the IEEE Analytic Methods for Power Systems (AMPS) technical committee. He has been an active contributor to several industry standardization efforts and technical working groups. Yanfeng is a senior member of IEEE and is a registered professional engineer (PE) in the state of Washington.

Gandhali Prakash Juvekar received her Bachelor of Technology in Electrical and Electronics Engineering from the National Institute of Technology Karnataka (NITK), India, in 2017. She received her MS in Electrical Engineering from Texas A&M University, College Station, TX, in 2019. She is currently a lead power engineer with Schweitzer Engineering Laboratories, Inc. (SEL). Her research interests include power system protection applications, time-domain quantities, geomagnetic disturbances, and distributed energy resources.

Normann Fischer received a Higher Diploma in Technology with honors from Technikon Witwatersrand, Johannesburg, South Africa, in 1988; a BSEE with honors from the University of Cape Town in 1993; an MSEE from the University of Idaho in 2005; and a PhD from the University of Idaho in 2014. He joined Eskom as a protection technician in 1984 and was a senior design engineer in the Eskom protection design department for three years. In 1999, Normann joined Schweitzer Engineering Laboratories, Inc. (SEL), where he is currently a vice president and distinguished engineer in the Research and Development division. He has authored and coauthored more than 80 technical papers and 12 transactions papers. He has more than 30 patents related to electrical engineering and power system protection. He is currently an IEEE Fellow and a member of the American Society for Engineering Education (ASEE).

Bill Glennon is a senior engineering director in the Research and Development division (R&D) at Schweitzer Engineering Laboratories, Inc. (SEL), where he leads the teams responsible for the product development of SEL distribution protection and control, fault indicators and sensors, and wireless product lines. Bill joined SEL in 2009 working in R&D on protective relay and recloser control design, development, and support in the distribution engineering group. In 2015, Bill joined the National Operations division, where he led technical sales activities for SEL in Montana and Wyoming for two years. He then served as the regional sales and service director for the Pacific Northwest U.S. and Western Canada region for four years before returning to R&D in his present role. He received his BS in electrical engineering from Montana Tech University and is an active member of IEEE.

Jesse Rorabaugh is a Senior Engineer at Southern California Edison working on grounding and wildfire mitigation. He received a bachelor’s degree at Fresno State, with a triple major in Physics, Chemistry, and Biology, a master’s degree at Cornell in Biomedical Engineering and a Professional Engineer license as an Electrical Engineer in the State of California. He is an active IEEE member and serves as chair for the G4 working group responsible for IEEE Std. 1246 and 1268 and vice chair for the G9 working group responsible for IEEE Std. 837.

Juan Santillan is a Senior Engineer at Southern California Edison (SCE) who works in the Protection Asset Engineering department. He is responsible for developing SCE Protection and Automation relay standards and supporting protection pilot projects for power system technologies and wildfire mitigation. He received his bachelor’s degree in electrical engineering from California State Polytechnic University, Pomona, and a Master’s in Power and Systems Engineering at California State University, Los Angeles. Before joining SCE, he gained extensive experience designing and executing industrial projects focusing on power system protection controls and automation.

Andrew Swisher is a Consulting Engineering at Southern California Edison. He attended California State Polytechnic University at Pomona where he earned a Bachelor’s of Science in Electrical and Computer Engineering with an emphasis in Power Systems Engineering. He is a registered professional engineer with the state of California and received his Master’s in Engineering from the University of Idaho in Moscow, ID along with the certificate for Power System Protection and Relaying.

20240911 • TP7161-01